Potential treatment benefits of a GLP-1R antagonist in combination with immune checkpoint inhibitors in colorectal cancer

ZENGQIN ZHAN[1], CHUNCHA ZHAN[2], LIANQIAO LI[1], DAN LAN[1], GUYA MENG[3] and FAN CHEN[1]

[1]Department of Oncology, Guangzhou Development District Hospital, Guangzhou, Guangdong 510700, P.R. China; [2]Department of General Practice, Tianyuan Community Health Service Center, Tianhe, Guangzhou, Guangdong 510000, P.R. China; [3]Department of Oncology, People's Hospital of Sandu County, Guizhou 558100, P.R. China

Received July 5, 2025; Accepted December 8, 2025

DOI: 10.3892/ol.2026.15485

Abstract. The clinical efficacy of immune checkpoint inhibitors (ICIs) in colorectal cancer (CRC) remains limited. Modulation of the glucagon-like peptide-1 receptor (GLP-1R) may enhance T-cell-mediated antitumor responses. The present study aimed to evaluate the antitumor effects of the GLP-1R antagonist Exendin 9-39 (Exe-9) combined with anti-programmed cell death protein-1 (PD-1) treatment in preclinical CRC models. Using *in vitro* co-culture assays, ELISA and *in vivo* murine models, alongside immunohistochemical and molecular analyses of clinical samples, HT-29 and MC38-OVA colon cancer cell lines were co-cultured *in vitro* with activated T cells in the presence of Exe-9. *In vivo*, male BALB/c mice were injected with MC38 to establish a CRC model and nude mice were used to assess T-cell dependency. To evaluate this synergistic effect, BALB/c mice with CRC were treated with Exe-9, anti-PD-1 or a combination. Additionally, clinical CRC samples were analyzed to assess the association of GLP-1R expression with the immunotherapy response. Exe-9 significantly enhanced T-cell-mediated cytotoxicity in CRC cell lines and reduced tumor growth in immunocompetent CRC mice; however, this effect was not observed in nude mice. Furthermore, combination therapy with the GLP-1R antagonist and anti-PD-1 yielded an improved antitumor effect compared with either treatment alone, and high GLP-1R ex2pression in clinical samples correlated with poor ICI response. These findings suggest that GLP-1R antagonism potentiates T-cell-mediated antitumor immunity and may provide a promising adjunctive therapeutic strategy for patients with CRC when combined with ICIs in the future.

Correspondence to: Dr Fan Chen, Department of Oncology, Guangzhou Development District Hospital, 39 Cuicheng North Street, Nanshitou Street, Haizhu, Guangzhou, Guangdong 510700, P.R. China
E-mail: 18011735931@163.com

Key words: colorectal cancer, glucagon-like peptide-1 receptor, Exendin 9-39, T-cell-mediated cytotoxicity, immune checkpoint inhibitors

Introduction

Colorectal cancer (CRC) is the third most common malignant tumor and the second leading cause of cancer-related death worldwide, ranking first in mortality among malignancies of the digestive system (1-4). The total number of mortalities from colon and rectal cancer is predicted to increase by 60.0 and 71.5%, respectively, when comparing between 2013 and the projection for 2035 (colon cancer: 158,816 vs. 254,165 cases; rectal cancer: 72,649 vs. 124,614 cases) (5). In China, the 5-year survival rate for patients with metastatic CRC is limited to 10-25% (6,7). Early-stage CRC can be treated with conventional modalities, such as surgical resection, chemotherapy and radiotherapy; these approaches usually yield limited efficacy and are associated with high recurrence rates (8), with >29% of CRC cases experiencing recurrence ≥5 years following primary surgical resection, while merely one-third of CRC cases are diagnosed at the localized stage (9,10) Recently, immune checkpoint inhibitors (ICIs), including anti-programmed cell death protein-1 (PD-1)/programmed death-ligand 1 (PD-L1) antibodies, have improved patient survival with several solid tumors, such as melanoma and lung cancer, by modulating the immune system to induce cytotoxic $CD8^+$ T cell-mediated tumor cell death (3,4,11,12). Despite the promise of immunotherapy as a potential treatment for CRC, its clinical success has been limited by factors such as aberrant signaling pathway activation leading to immune evasion, impaired antigen presentation and accumulation of immunosuppressive cells (5,6,13,14). This challenge is particularly evident in microsatellite-stable CRC, where a low tumor mutation burden and a paucity of neoantigens render immunotherapy less effective (7,15). Therefore, novel combinatorial treatment strategies are urgently needed to enhance the immune response in patients with CRC.

The glucagon-like peptide-1 receptor (GLP-1R) is primarily expressed on pancreatic β-cells, serves a key role in regulating blood glucose levels and metabolism

through its specific interaction with GLP-1 (8,16). Initially, the research focused on treating diabetes and cardiovascular diseases (9,10,17,18); however, GLP-1R agonist therapies indirectly alleviate hepatic inflammation and fibrosis, offering benefits for the management of metabolic liver diseases (11,19). Recent studies have highlighted the potential of targeting GLP-1R beyond conventional metabolic endpoints, such as gastrointestinal stress attenuation and pain modulation (20-22). Notably, emerging evidence indicates that GLP-1R activation modulates various innate immune cells, including macrophages and innate-like T lymphocytes (23-25) Furthermore, several T cell subsets express functional GLP-1R in animal models and human participants, underscoring its notable role in immune regulation (26). In preclinical murine CRC models, GLP-1R has been shown to be a negative co-stimulatory molecule that dampens T-cell function and attenuates graft immune responses, whereas GLP-1R antagonists provoke robust antitumor immunity. Collectively, these findings suggest that the immunomodulatory properties of GLP-1R have potential for the development of innovative cancer immunotherapy strategies in the future.

Due to the potential of GLP-1R antagonists to modulate T-cell regulation and the evidence that enhancing T-cell infiltration can effectively transform 'cold' tumors into 'hot' tumors (27-29), it is plausible that combining GLP-1R antagonists with ICIs may synergistically modulate T-cell-mediated immune sensitivity to improve tumor treatment outcomes. However, current investigations into GLP-1R in patients with cancer have predominantly focused on its role in mitigating cardiovascular complications or their side effects (30,31). For example, a retrospective cohort study indicated that GLP-1RAs may help alleviate cardiac dysfunction caused by anticancer treatments, such as chemotherapy or radiotherapy (32). Common side effects of GLP-1RAs, including semaglutide, involve gastrointestinal reactions such as nausea and vomiting. Further research suggested that simultaneous activation of the glucose-dependent insulinotropic polypeptide receptor may mitigate these adverse effects through an anti-emetic mechanism (33). The potential antitumor benefits of combining GLP-1R antagonism with immune checkpoint inhibition in CRC remain to be explored.

In the present study, the effects of the GLP-1R antagonist Exendin 9-39 (Exe-9) on T-cell function, $CD8^+$ T cell-mediated tumor cell killing and the synergistic antitumor efficacy of its combination with ICIs were systematically evaluated via *in vitro* co-culture systems and *in vivo* CRC mouse tumor models. Furthermore, the relationship between GLP-1R expression levels and immunotherapy response was analyzed in samples of patients with CRC to assess its potential as a predictive clinical outcomes biomarker. Therefore, the present study aimed to provide experimental evidence for the combined application of GLP-1R antagonists and ICIs in CRC, offering novel strategies for optimizing combination therapies for this disease in the future.

Materials and methods

Ethics statement. All experimental procedures involving animals and human tissues were approved by the Ethics Committee of Guangzhou Development District Hospital (approval no. F2024-030; Guangzhou, China).

All animal experiments were approved by the Institutional Animal Care and Use Committee of Guangzhou Development District Hospital (Guangzhou, China). Mice were housed in a specific pathogen-free facility, maintained in a controlled environment (22±2˚C, 50 ± 10% humidity, 12 h light/dark cycle) and provided *ad libitum* access to food and water. All efforts were made to minimize animal suffering. For human studies, this research utilized a retrospective design. Peripheral blood samples were retrospectively collected from healthy donors, and matched tumor tissue samples were obtained from patients with CRC, respectively, following the provision of written informed consent in accordance with the Declaration of Helsinki. The study protocol, including the retrospective use of these samples, was approved by the Institutional Review Board of the Guangzhou Development District Hospital (Guangzhou, China).

Clinical sample collection and grouping. Peripheral blood samples were collected from healthy donors via venipuncture and drawn into sterile ethylenediaminetetraacetic acid-coated tubes on ice. Clinical tumor specimens were collected from 11 patients with colon cancer who received ICI therapy at Guangzhou Development District Hospital (Guangzhou, China) between July 2022 and December 2024. Patients were enrolled based on the following criteria: i) Histologically confirmed diagnosis of colon adenocarcinoma; ii) scheduled to undergo or having undergone first-line ICI therapy (either as monotherapy or in combination); iii) availability of pre-treatment tumor tissue samples and complete clinical follow-up records; iv) aged ≥18 years. Key exclusion criteria included: i) Prior history of other active malignancies ≤5 years; ii) severe concurrent autoimmune diseases or active infections; iii) receipt of any other form of anticancer therapy (such as chemotherapy or radiotherapy) ≤4 weeks prior to sample collection; v) incomplete clinical or pathological data. Surgical resection or core needle biopsy was used to obtain tumor tissues, which were immediately placed in ice-cold RPMI-1640 medium (Gibco; Thermo Fisher Scientific, Inc.). Based on the Response Evaluation Criteria for Solid Tumors (34), tumor responses were evaluated using contrast-enhanced computed tomography. Patients whose target lesions exhibited either complete response (CR) or partial response (PR) were categorized as responders (n=5), whereas those with stable disease (SD) or progressive disease (PD) were classified as non-responders (n=6). CR was defined as the disappearance of all target lesions and PR as a ≥30% reduction in their total diameter. SD was characterized by insufficient shrinkage to qualify as a partial response and PD was defined as a minimum 20% increase in the target lesions. The clinical cohort consisted of 7 men and 4 women, with a median age of 62 years (range, 48-71 years).

Cell maintenance and treatment. The CRC cell lines MC38 (cat. no. iCell-m032; Mirror Point (Shanghai) Cell Technology Co., Ltd) and HT-29 (cat. no. iCell-h078; Mirror Point (Shanghai) Cell Technology Co., Ltd) were maintained according to the manufacturer's protocols. They were cultured with activated T cells (specifically, *in vitro*-activated human peripheral blood-derived T cells and isolated murine $CD8^+$

T cells from OT-1 mice, as detailed in the 'T-cell separation' section) at 37˚C in a 5% CO_2 incubator. MC38 cells were genetically modified to overexpress SIINFEKL via a lentiviral vector system (cat. no. MC38-OVA; iCell Biotech). Cells were cultured in DMEM (Gibco; Thermo Fisher Scientific, Inc.), supplemented with 10% fetal bovine serum (FBS; Gibco; Thermo Fisher Scientific, Inc.), 100 U/ml penicillin, 100 μg/ml streptomycin and maintained in a humidified incubator at 37˚C with 5% CO_2. For the treatment experiments, cells were either cultured individually or co-cultured with activated T cells at a ratio of 3:1 for 48 h in the presence of Exe-9 (GLP-1R antagonist; cat. no. E7269; MilliporeSigma) at concentrations of 10 and 50 nM, whereas parallel cultures received phosphate-buffered saline (PBS) as the vehicle control.

T-cell separation. Human peripheral blood mononuclear cells were isolated from whole blood of healthy donors via density gradient centrifugation using Lymphoprep (cat. no. 10970; STEMCELL Technologies). Specifically, blood was collected in BD CPT tubes (cat. no. 362782; BD Biosciences) containing Ficoll™ density gradient medium (P=1.077 g/cm^3) and sodium citrate. Tubes were incubated at room temperature for 20 min to stabilize the temperature, then centrifuged at 1,650 x g for 20 min at 20˚C with the brake on. This formed a density barrier separating PBMCs and serum. The PBMC fraction was gently mixed with the serum by inversion and transferred to 15 ml tubes for further processing. and subsequently cultured in CTS™ AIIM V™ SFM medium (cat. no. A3021002; Gibco; Thermo Fisher Scientific, Inc.) supplemented with ImmunoCult™ Human CD3/CD28/CD2 T Cell Activation Reagent (cat. no. 10970; STEMCELL Technologies) and recombinant 1,000 U/ml human interleukin (IL)-2 (cat. no. 11848-HNAY1; Sino Biological, Inc.) for 7 days to obtain activated human T cells. $CD8^+$ T cells were isolated from the spleens of OT-1 mice (cat. no. 003831; THE JACKSON LABORATORY), aged 6-8 weeks old with a body weight of 18-25 g using the EasySep™ Mouse $CD8^+$ T Cell Isolation Kit (STEMCELL Technologies) in accordance with the manufacturer's instructions. Collected cells were cultured briefly in complete T cell medium comprising RPMI-1640 (Gibco; Thermo Fisher Scientific, Inc.) supplemented with 10% FBS, 20 mM HEPES, 1 mM sodium pyruvate, 0.05 mM 2-mercaptoethanol, 2 mM L-glutamine and 50 U/ml streptomycin/penicillin, with recombinant mouse IL-2 (cat. no. CK24; Novoprotein Scientific, Inc.) and incubated for 5 days.

Cell viability assay. After treatment, the adherent cancer cells were washed thrice with PBS, fixed with 100% methanol at room temperature for 10 min and stained with a 0.5% crystal violet solution at room temperature for 30 min. After staining, the wells were rinsed with PBS to remove excess dye and subsequently solubilized by adding 10% acetic acid for 10 min. Optical density (OD) was measured at 570 nm using a BioTek Epoch 2 microplate reader (BioTek Instruments; Agilent Technologies, Inc.) to quantitatively determine cell viability.

Cytokine quantification. To quantify interferon (IFN)-γ and tissue necrotic factor (TNF)-α levels, the supernatants of the colon cancer cell culture were collected after a 48 h incubation period at 37˚C and centrifuged at 13,000 x g for 5 min at 4˚C. The supernatants were analyzed using the Mouse IFN-γ enzyme-linked immunosorbent assay (ELISA) Kit (cat. no. PI508; Beyotime Biotechnology), Mouse TNF α ELISA Kit (cat. no. ab285327; Abcam), Human IFN-γ ELISA Kit (cat. no. PI521; Beyotime Biotechnology) and human TNF α ELISA Kit (cat. no. ab181421; Abcam), in strict accordance with the manufacturer's instructions. Briefly, 100 μl each standard and sample was dispensed into pre-coated wells of a 96-well microplate and incubated for 2 h at room temperature. After washing with 0.05% Tween-20 in PBS, 100 μl horseradish peroxidase (HRP)-conjugated detection antibody (provided within the respective ELISA kits was added.

The antibody in the aforementioned IFN-γ reagent kit was used directly (utilizing the pre-prepared formulation provided with the kit, which required no additional dilution), while the antibody in the TNF-α reagent kits was used at a 1:100 dilution; both antibody application protocols followed the specifications in the respective manufacturers' instructions; cat. no. 80220; Alpha Diagnostic Intl. Inc.) was added and the plate was incubated for an additional 1 h at room temperature. After a series of washes, 100 μl tetramethylbenzidine substrate solution (MilliporeSigma) was added and the enzymatic reaction proceeded in the dark for 20 min. The reaction was terminated by the addition of 50 μl 2 M sulfuric acid and the absorbance was measured at 450 nm. Cytokine concentrations were determined by generating standard curves using recombinant cytokine standards provided in the kits.

Animal experiment. Male BALB/c mice (6-8 weeks old; 22-25 g) were purchased from Beijing Vital River Laboratories Animal Technology Co., Ltd. and subcutaneously injected with 1x10^6 MC38 cells (day 0) into the left flank. When tumor volumes reached ~150 mm^3, the mice were randomized into treatment groups (n=10). To assess the antitumor efficacy of Exe-9, mice were randomly allocated to either the Exe-9 group (n=10) or the control group (n=10). To evaluate the synergistic effect of Exe-9 combined with Anti-PD-1, mice were randomly assigned to four groups: Control (n=10), Exe-9 (n=10), Anti-PD-1 (n=10) and Exe-9 + Anti-PD-1 (n=10). Mice in the Exe-9 group received intratumoral injections of Exe-9 at a concentration of 25 nmol/kg in saline on days 10, 12, 14 and 16. Mice in the Anti-PD-1 group were administered 100 μg of anti-PD-1 antibody (cat. no. BE0146; Bio X Cell, Lebanon) via intraperitoneal injection on days 10, 13, 16 and 19. The control mice received equivalent volumes of sterile saline or isotype immunoglobulin G (IgG; cat. no. 1054; Bio X Cell), as appropriate. To further elucidate whether the antitumor effects of Exe-9 were mediated by the modulation of tumor immunity, an additional experiment was conducted in male BALB/c nude mice (Beijing Vital River Laboratories Animal Technology Co., Ltd.) using the same group size (n=10 per group) following the same injection schedule as the Exe-9 group.

Prior to the invasive procedures, the mice were anesthetized via inhalation of isoflurane (3-4% for induction and 1.5-2% for maintenance in oxygen). Mice demonstrating severe distress signs at the end of the experiment were humanely euthanized via CO_2 inhalation, followed by cervical dislocation.

Tumor length and width were recorded at the same intervals as the injections using digital calipers to generate tumor growth curves. According to institutional ethical guidelines,

the maximum tumor volume permitted was 1,500 mm^3 and the maximum diameter did not exceed 20 mm in any dimension. In the present study, the largest tumor measured was ~1,200 mm^3 in volume and 17 mm in diameter. The mice were euthanized on day 20; tumor tissue and spleen were collected for further assays. Euthanasia was performed by gradual CO_2 inhalation at a displacement rate of 30-40% volume per min of the chamber, followed by cervical dislocation to ensure mortality. The tumors were harvested and weighed to assess their anticancer efficacy every 2 days starting from day 10.

Immunohistochemistry (IHC). Excised mouse or patient tumor tissues were fixed in 10% neutral-buffered formalin for 24 h at room temperature and processed for paraffin embedding. Paraffin blocks were sectioned at 5 μm thickness and mounted onto slides. Sections were deparaffinized in xylene and rehydrated using a graded ethanol series (100, 95 and 70%) before rinsing in distilled water. After heating in a 10 mM citrate buffer (pH 6.0) at 92˚C for 15 min, slides were incubated in 3% hydrogen peroxide for 10 min at room temperature. For the detection of the intracellular/membrane protein GLP-1R, sections were permeabilized with 0.1% Triton X-100 in PBS for 10 min at room temperature. Blocking was performed with 5% normal goat serum (cat. no. 5425; Cell Signaling Technology, Inc.) for 30 min at room temperature and the sections were incubated overnight at 4˚C with a primary anti-CD8 (cat. no. PA007381.r2b; Syd Labs) or anti-GLP-1R antibody (cat. no. EPR21819; Abcam) diluted 1:100 in blocking solution. After three washes in PBS, a biotinylated goat anti-mouse IgG secondary antibody (1:200; cat. no. ab6789; Abcam), was applied for 1 h at room temperature. Immunoreactivity was visualized using the VECTASTAIN® Elite ABC HRP Kit (Vector Laboratories, Inc.) with diaminobenzidine, following the manufacturer's protocol. Subsequently, the sections were counterstained with hematoxylin (MilliporeSigma) at a concentration of 1% for 2 min at room temperature, dehydrated using graded ethanol and xylene solutions and cover slipped. The stained slides were examined and imaged under an Olympus BX53 light/fluorescence microscope (Olympus Corporation). Quantitative analysis of IHC staining was performed using the Alpathwell Pathology Image Analysis System (version 3.5; Servicebio Technology Co., Ltd.).

GLP-1R staining was semi-quantified using the H-score method (35). For each case, five tumor fields (x400 magnification) were randomly selected within the tumor area. The percentage of tumor cells demonstrating weak (1+), moderate (2+) or strong (3+) staining intensity was recorded (P1-P3; total, 0-100%) and the H-score was calculated as (1xP1 + 2xP2 + 3xP3), yielding a range of 0-300. Two board-certified pathologists independently scored all slides in a blinded manner. In cases of initial disagreement, the two pathologists first re-examined the corresponding slides together to reach a consensus. If a consensus could not be achieved, a third senior pathologist was consulted to make the final determination.

Enzyme-linked immunosorbent spot (ELISpot) assay. Spleens harvested from Exp-9 treated mice or the naive control were mechanically dissociated and filtered through a 70 μm cell strainer to obtain a cell suspension. Cells were then plated at a density of $1x10^5$ cells per well in ELISpot plates pre-coated with anti-IFN-γ capture antibody, as provided in the Mouse IFN-γ ELISpot Kit (cat. no. 3321-4APT-2; Mabtech). For restimulation, cells were incubated with either irradiated MC38 cells or the major histocompatibility complex (MHC)-I restricted AH1 peptide derived from MC38 cells (MilliporeSigma) at a final concentration of 1 μg/ml. After being cultured for 20 h at 37˚C, the plates were washed with PBS and incubated with a biotinylated anti-IFN-γ detection antibody for 2 h at room temperature. After subsequent washing steps, an HRP conjugate was added and the reaction was developed using a 3-amino-9-ethylcarbazole substrate solution (cat. no. SK-4200; Vector Laboratories, Inc.) at room temperature in the dark for 15 min. The enzymatic reaction was stopped by rinsing the plates with distilled water and the spots were counted using an automated ELISpot reader (ELR08; Cellular Technology Limited).

Reverse transcription (RT)-quantitative PCR. Total RNA was extracted from freshly frozen tissue samples using TRIzol® reagent (Invitrogen; Thermo Fisher Scientific, Inc.), following the manufacturer's instructions. RNA purity and concentration was assessed using a NanoDrop™ 2000 spectrophotometer (Thermo Fisher Scientific, Inc.). Subsequently, 1 μg total RNA was reverse transcribed into cDNA using the PrimeScript™ RT reagent Kit (Takara Bio, Inc.). The quantitative real-time PCR was performed on an ABI 7500 Real-Time PCR System (Applied Biosystems, Inc.; Thermo Fisher Scientific, Inc.) using SYBR® Premix Ex Taq II (Takara Bio, Inc.) The PCR protocol comprised three stages: Initial denaturation at 95˚C for 30 sec to activate the DNA polymerase and denature templates; 40 cycles of amplification, each consisting of denaturation at 95˚C for 5 sec followed by a combined annealing/extension at 60˚C for 30 sec (the temperature of this step was optimized based on the primer Tm); and a melting curve analysis (95˚C for 15 sec; 60˚C for 1 min; then gradual heating to 95˚C) to confirm amplicon specificity and exclude nonspecific products. The primers used to detect GLP-1R and GAPDH for normalization are listed in Table SI. PCR conditions were set as: 95˚C for 30 sec, followed by 40 cycles of 95˚C for 5 sec and 60˚C for 30 sec. Relative gene expression was calculated using the $2^{-\Delta\Delta Cq}$ method (36). All primers were designed for human genes and validated by National Center for Biotechnology Information Basic Local Alignment Search Tool (National Institutes of Health).

Western blotting analysis. Tissue samples from patients with CRC were homogenized and lysed using radioimmunoprecipitation assay buffer supplemented with 1% protease inhibitor cocktail and 1% phosphatase inhibitor cocktail (MilliporeSigma) on ice for 30 min. Lysates were clarified via centrifugation at 12,000 x g for 15 min at 4˚C and protein concentrations were determined using a BCA protein assay kit (Thermo Fisher Scientific, Inc.). Equal amounts of proteins (30 μg per lane) were resolved on 10% sodium dodecyl sulfate-polyacrylamide gel electrophoresis gels and transferred onto polyvinylidene difluoride membranes

(MilliporeSigma) using a Bio-Rad Trans-Blot Turbo system. The membranes were blocked with 5% (w/v) skim milk in Tris-buffered saline containing 0.1% Tween-20 (TBST) for 1 h at room temperature. Membranes were incubated overnight at 4˚C with primary antibodies targeting GLP-1R (1:500). After washing, the membranes were incubated with HRP-conjugated secondary IgG (1:2,000, Beyotime Biotechnology) for 1 h at room temperature. Protein bands were visualized using an enhanced chemiluminescence detection kit (Thermo Fisher Scientific, Inc.) and imaged using the ChemiDoc XRS+ Imaging System (Bio-Rad Laboratories, Inc.). Densitometric band intensity analysis was performed using the ImageJ 2.0 software (National Institutes of Health), with GAPDH used for normalization. The antibodies used for western blotting analysis are listed in Table SII.

Statistical analysis. All data were analyzed using the GraphPad Prism software (version 9.0; Dotmatics). Continuous variables were expressed as mean ± SEM and the Shapiro-Wilk test was employed to assess data normality. For normally distributed data, one-way ANOVA followed by Tukey's honest significant difference post hoc test was used for group comparisons, whereas for non-normally distributed data, the Kruskal-Wallis test with Dunn's multiple comparison test was applied. Pearson's correlation analysis was performed to evaluate the correlation between tumor volume and the number of IFN-γ-secreting cells, as well as between GLP-1R expression and the immunotherapy response. $P<0.05$ was considered to indicate a statistically significant difference.

Results

GLP-1R antagonist potentiates T-cell-mediated cytotoxicity against colon cancer cells. The colon cancer cell lines HT-29 and MC38-OVA were cultured either individually or co-cultured with activated T cells for 48 h in the presence of the GLP-1R antagonist Exe-9 at 10 or 50 nM or PBS as the vehicle control. The viability of HT-29 (Fig. 1A) and MC38-OVA (Fig. 1B) cells was assessed. In the absence of T cells, Exe-9 treatment did not significantly alter cancer cell viability, as no statistically significant differences were detected between the PBS- and Exe-9-treated groups. By contrast, when co-cultured with activated T cells, a significant dose-dependent reduction in cell viability was observed, indicating enhanced T-cell-mediated cytotoxicity in the presence of Exe-9. In parallel, ELISA measurements of the culture supernatants revealed that levels of IFN-γ (Fig. 1C) and TNF-α (Fig. 1D) increased following Exe-9 treatment compared with the control, with a dose-dependent effect evident particularly in the MC38-OVA cultures. Collectively, these results suggest that Exe-9 enhances the killing efficiency of $CD8^+$ T cells against colon cancer cells, potentially by modulating the cytokine milieu that governs T-cell-mediated cytotoxicity.

GLP-1R antagonist enhances T-cell-mediated antitumor efficacy in mice. To evaluate the effects of the GLP-1R antagonist on tumor growth, male mice were subcutaneously injected with MC38 tumor cells. When tumors reached ~150 mm^3 on day 10, Exe-9 was administered intratumorally at days 10, 12, 14 and 16, while control mice received equivalent volumes of saline. Tumor tissues were collected on day 20 for analysis (Fig. 2A). Notably, the tumors in Exe-9-treated mice were markedly smaller compared with those in the control group (Fig. 2B). The tumor volume measurements recorded at each treatment point demonstrated a continuous increase in both groups. However, the Exe-9 group exhibited a markedly lower growth rate (Fig. 2C) compared with the control group. At the endpoint, tumor volume (Fig. 2D) and weight (Fig. 2E) in the control group were significantly greater compared with those in the Exe-9-treated group. IHC analysis revealed that tumors from Exe-9-treated mice displayed markedly higher $CD8^+$ T-cell infiltration compared with those from the control group (Fig. 2F), suggesting enhanced antitumor immunity. To investigate the role of T cells in this response, the experiment was replicated using nude mice lacking functional T cells. In this model, no significant differences in tumor size were observed between the Exe-9 and saline-treated groups (Fig. 2G); however, the tumor volume continued to increase in both groups throughout the treatment period (Fig. 2H and I). Tumor weights collected on day 20 were also not significantly different between the two groups (Fig. 2J). These findings suggested that the antitumor effects of Exe-9 depend on the presence of functional T cells, potentially through the enhancement of $CD8^+$ T-cell-mediated immunity.

GLP-1R antagonist elicits tumor-specific $CD8^+$ T-cell replication. To investigate the effect of the GLP-1R antagonist on tumor-specific $CD8^+$ T-cell responses, splenocytes were collected from mice and restimulated for 20 h with either MC38 tumor cells or MHC-I-restricted AH1 peptide. The number of IFN-γ-secreting cells was quantified using ELISpot assays. Exe-9-treated mice exhibited significantly higher numbers of IFN-γ-secreting cells compared with the control mice under MC38 (Fig. 3A) and AH1 (Fig. 3B) restimulation conditions. Correlation analysis between tumor volume and IFN-γ-secreting cells revealed distinct patterns. In the Exe-9-treated group, a negative correlation trend was observed between them following MC38 restimulation, although the trend was not statistically significant ($r=-0.6302$; $P=0.0508$; Fig. 3C). However, a significant negative correlation was identified when the AH1 peptide was restimulated ($r=-0.6439$; $P=0.0445$; Fig. 3D), suggesting that Exe-9 treatment enhanced tumor-specific $CD8^+$ T-cell activation. By contrast, splenocytes of mice from the control group consistently exhibited low numbers of IFN-γ-secreting cells, regardless of tumor volume or type of restimulation antigen (Fig. 3C and D). These results revealed that Exe-9 promotes the generation of tumor-specific $CD8^+$ T cells capable of robust IFN-γ production. These results further suggest that the enhanced antitumor response induced by Exe-9 is likely mediated by an increase in antigen-specific $CD8^+$ T-cell activity.

Combination of GLP-1R antagonist and ICIs synergistically suppresses colon cancer growth in vivo. A combination treatment experiment with a GLP-1R antagonist and an ICI was performed in mice bearing MC38 tumors. Tumors were established to an average volume of ~150 mm^3 by day

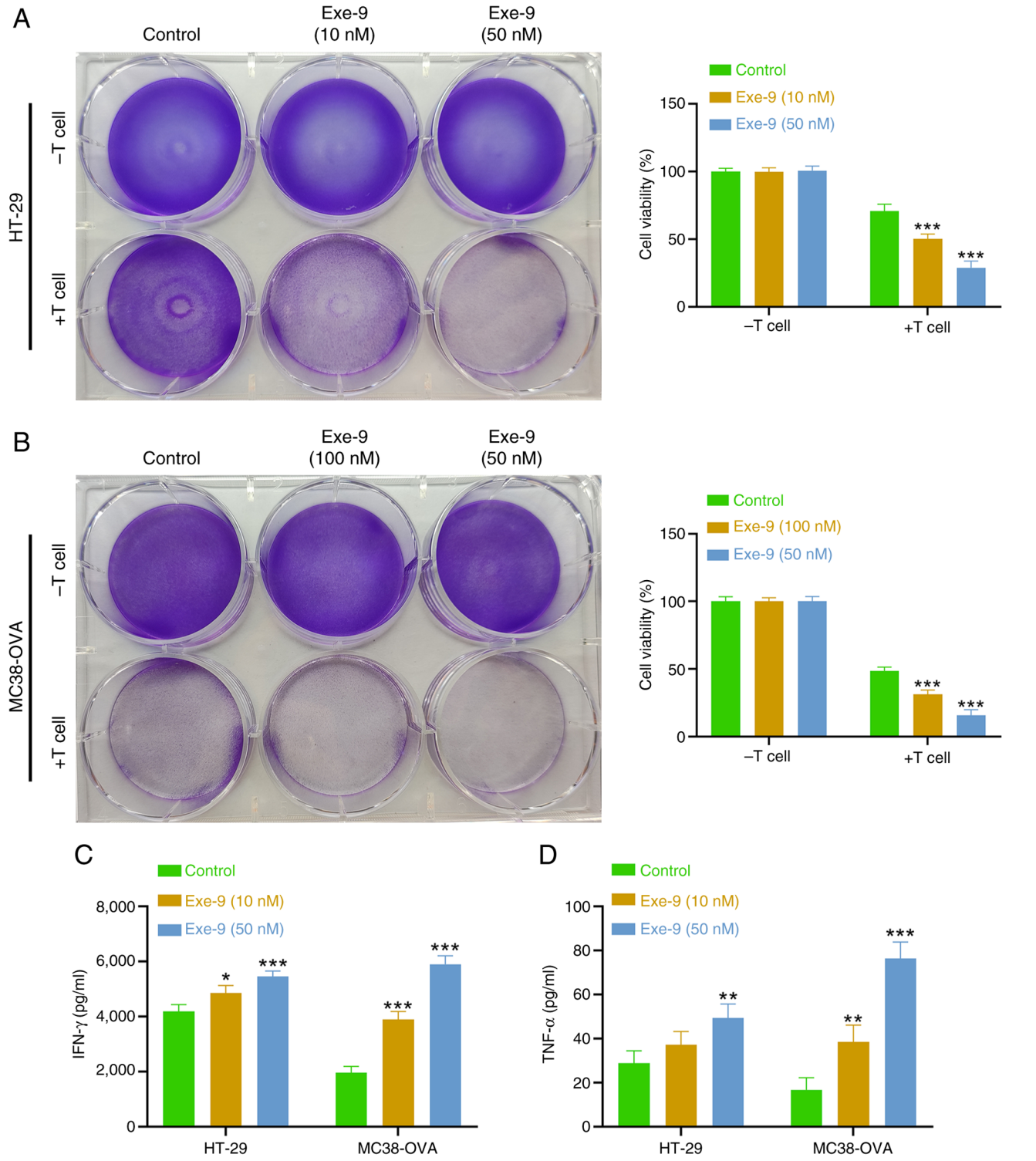

Figure 1. Glucagon-like peptide-1 receptor antagonist enhances T-cell-mediated cytotoxicity against colon cancer cells. Colon cancer cell lines HT-29 and MC38-OVA were cultured either individually or co-cultured with activated T cells for 48 h in the presence of Exe-9 at concentrations of 10 and 50 nM. (A) Viability of HT-29 colon cancer cells cultured alone or in co-culture with activated T cells for 48 h, treated with Exe-9 (10 or 50 nM) or control. Viability was assessed by crystal violet staining; quantitative spectrophotometric data are shown (right panel); (B) viability of MC38-OVA colon cancer cells under the same culture and treatment conditions as in, (A) quantified by crystal violet staining (right panel, spectrophotometric data); (C) IFN-γ levels in culture supernatants from the 48-h co-cultures described in (A) and (B), measured by ELISA; (D) TNF-α levels in the same supernatants as in (C), determined by ELISA. *P<0.05, **P<0.01 and ***P<0.001. Exe-9, Exendin 9-39; IFN-γ, interferon-γ; TNF-α, tumor necrosis factor-α.

10 post-injection. Mice were treated intratumorally with Exe-9 on days 10, 12, 14 and 16 or injected intraperitoneally with anti-PD-1 on days 10, 13, 16 and 19. A combination of both treatments or a control with saline and IgG, was administered at the same time points. The tumors were collected on day 20 for further analysis (Fig. 4A). The control group exhibited the largest tumors, followed by the Exe-9, then the Anti-PD-1 group and the Exe-9 + Anti-PD-1

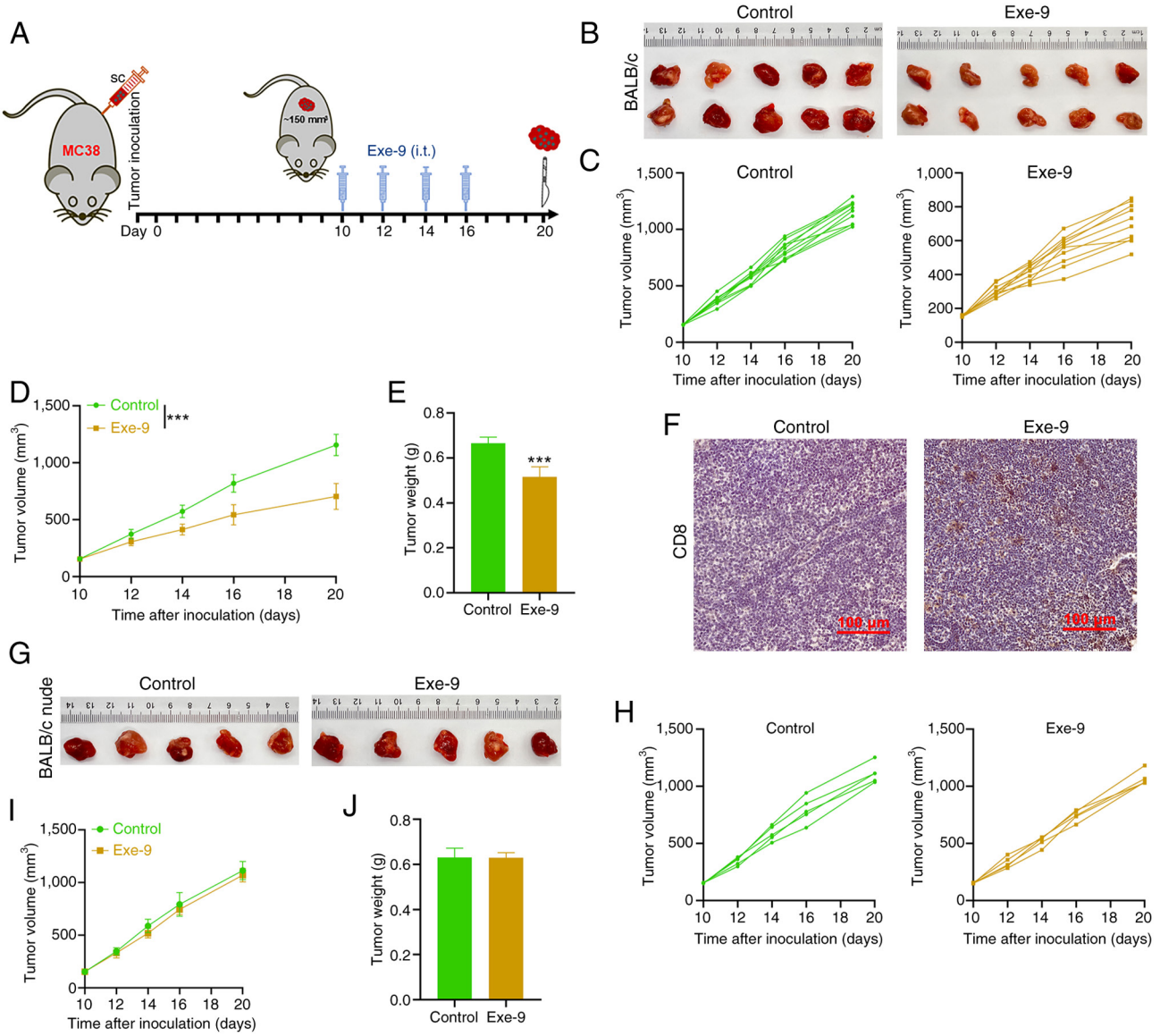

Figure 2. Glucagon-like peptide-1 receptor antagonist enhances T-cell-mediated antitumor efficacy in mice. (A) A schematic representation of the experimental timeline. Mice were subcutaneously injected with MC38 tumor cells to generate a colorectal cancer model, after which Exe9 was administered intratumorally on days 10, 12, 14 and 16. (B) Representative images of excised tumor tissues collected on day 20. (C) Tumor volumes were measured at regular intervals during the treatment period. (D) Endpoint tumor volumes and (E) tumor weights are depicted to illustrate the difference between groups. (F) Immunohistochemical analysis was conducted to assess the infiltration of $CD8^+$ T cells in tumor sections (scale bar, 100 μm). (G) In a parallel study using nude mice, tumor volumes of (H) individual mice and (I) their average value and (J) tumor weights, were similarly measured to determine the dependence of the antitumor effects on T-cell-mediated immunity. Data are presented as mean ± SEM. ***P<0.001. SC, subcutaneous; Exe-9, Exendin 9-39; i.t., intratumoral injections.

group with the smallest tumors (Fig. 4B). While the tumor volumes in the control, Exe-9 and Anti-PD-1 groups continuously increased throughout the treatment period, the combination of Exe-9 and Anti-PD-1 resulted in effective tumor control, with no significant changes in tumor volume observed (Fig. 4C). By day 20, the tumor volumes were quantified as shown in Fig. 4D and revealed the same trend as shown in the representative images in Fig. 2B. Consistent with these observations, the tumor weights at the endpoint also demonstrated significant differences among groups. Specifically, the tumor weight in the combination treatment group (Exe-9 + Anti-PD-1) was significantly reduced compared with that in the Anti-PD-1 monotherapy group (P<0.001; Fig. 4E). These results illustrate that Exe-9 enhanced the antitumor efficacy of anti-PD-1 *in vivo*, indicating a potential synergistic interaction between GLP-1R antagonism and immune checkpoint inhibition in suppressing colon cancer growth.

High expression of GLP-1R correlates with reduced efficacy of anti-PD-1 immunotherapy. To investigate the clinical relevance of GLP-1R expression in tumor immunotherapy, tumor samples from 11 patients with CRC treated with ICIs were collected and categorized into responder and non-responder groups based on therapeutic outcomes. Quantitative PCR analysis revealed that GLP-1R expression levels were significantly higher in tumor tissues from non-responders compared with those from responders (P<0.05; Fig. 5A). Stratifying patients into high and low GLP-1R expression groups based on the median expression

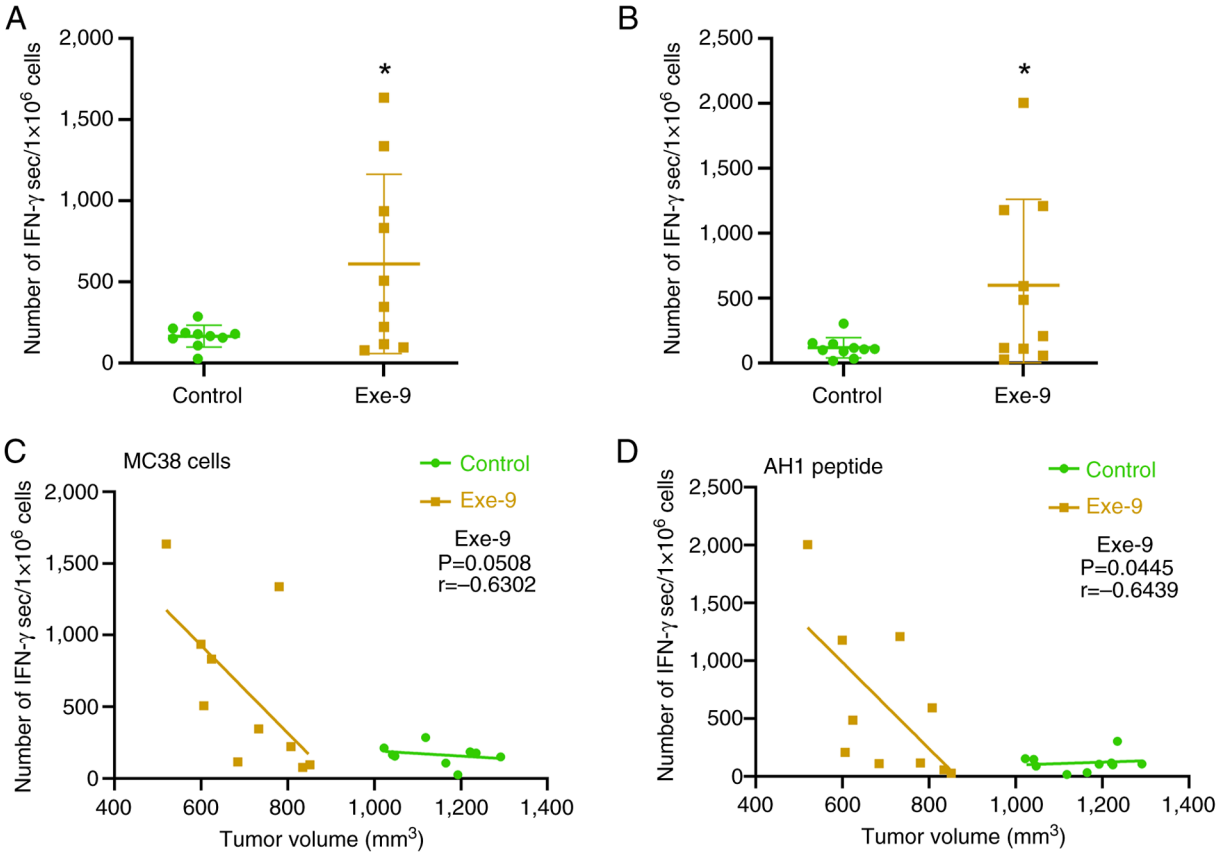

Figure 3. Glucagon-like peptide-1 receptor antagonist induces tumor-specific CD8+ T-cell replication. (A) Number of IFN-γ-secreting cells quantified by ELISpot after restimulation of splenocytes from Exe-9-treated mice with MC38 tumor cells for 20 h; (B) number of IFN-γ-secreting cells quantified by ELISpot after restimulation of splenocytes from Exe-9-treated mice with the MHC-I-restricted AH1 peptide for 20 h; (C) Pearson correlation between the number of IFN-γ-secreting cells (from MC38-restimulated group) and tumor volume; (D) Pearson correlation between the number of IFN-γ-secreting cells (from AH1 peptide-restimulated group) and tumor volume. Data are presented as mean ± SEM. *P<0.05. Exe-9, Exendin 9-39; sec, secreting; IFN-γ, interferon-γ.

level revealed a positive correlation between high GLP-1R expression and non-responsiveness to therapy (r=0.8718; P=0.0005; Fig. 5B). These findings were corroborated by IHC and western blotting analyses, revealing that GLP-1R protein expression was significantly higher in tumor tissues from non-responders compared with those from responders (Fig. 5C and D). These results indicate that elevated GLP-1R expression is associated with reduced efficacy of anti-PD-1 immunotherapy in patients with CRC.

Discussion

The incidence of CRC is rapidly increasing and is associated with high mortality. However, the clinical efficacy of ICIs remains limited, highlighting the urgent need to explore novel complementary therapeutic strategies (37). In the present study, a multitiered experimental approach was employed to comprehensively assess the application of the GLP-1R antagonist Exe-9 and its potential as an adjunct in CRC immunotherapy.

GLP-1R antagonists competitively occupy the binding site of GLP-1R, inhibiting downstream GLP-1 signal transduction. *In vitro* experiments revealed that under co-culture conditions with activated T cells, Exe-9 significantly decreased cancer cell viability in a dose-dependent manner, whereas no cytotoxic effect was observed in the absence of T cells. This finding was corroborated by *in vivo* studies using a CRC mouse model in which BALB/c mice treated with Exe-9 exhibited significantly attenuated tumor growth and increased intratumoral infiltration of CD8+ T cells, which were absent in nude mice lacking functional T cells. These results indicate that the cytotoxic effects induced by GLP-1R antagonism were mediated by T-cell activity. This observation is consistent with previous reports revealing that GLP-1R signaling exerts a negative modulatory effect on T-cell function and antagonism of this receptor can potentiate antitumor immune responses (38,39).

However, other studies have reported conflicting findings regarding the role of GLP-1R in tumor biology, reflecting its diverse functions across various cancer types, experimental models and immune microenvironments. For instance, the GLP-1R agonist semaglutide promotes tumor cell proliferation in neuroendocrine cancer (40), whereas a meta-analysis encompassing eight original studies revealed that GLP-1R agonists may confer protective effects against liver cancer (24,41). Furthermore, in CRC cell lines, GLP-1R activation inhibits tumor cell proliferation (42). These discrepancies underscore the complex and context-dependent nature of GLP-1R signaling. The present study provided direct laboratory evidence supporting the antitumor effects of GLP-1R antagonism in CRC, as opposed to agonism; however, further investigations are warranted. Future researchers should aim to delineate the regulatory mechanisms and dose-response

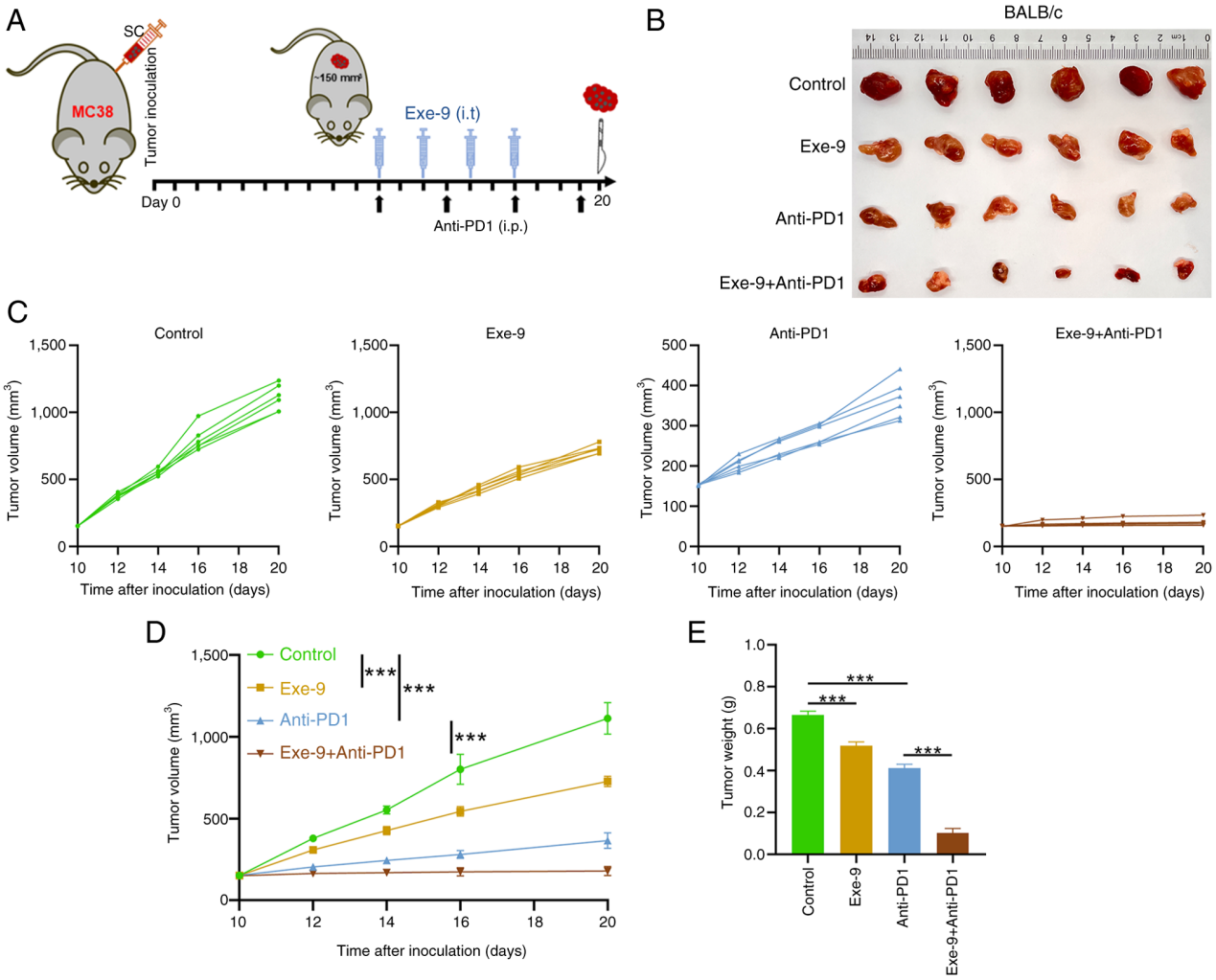

Figure 4. A combination of glucagon-like peptide-1 receptor antagonist and immune checkpoint inhibitors synergistically suppresses colorectal cancer growth *in vivo*. Mice bearing MC38 tumors were administered intratumoral injections of the glucagon-like peptide-1 receptor antagonist Exe-9 on days 10, 12, 14 and 16 or intraperitoneal injections of the anti-PD-1 antibody on days 10, 13, 16 and 19 or both treatments as the (A) schematic representation of experimental design demonstrates. (B) Representative excised tumor images collected on day 20 post-treatments. (C) Tumor growth curves during the treatment period generated by regular measurements of tumor dimensions using digital calipers. (D) Tumor volumes and (E) weights quantified at the endpoint. Data are presented as mean ± SEM. ***P<0.001. Exe-9, Exendin 9-39; PD-1, programmed cell death protein-1; SC, subcutaneous; i.t., intratumoral injections; i.p., intraperitoneal.

relationships of the GLP-1R pathway under more refined experimental conditions, facilitating the development of precise immunotherapeutic strategies.

Furthermore, Exe-9 treatment was associated with a dose-dependent increase in tumor cell death, concomitant with an increase in IFN-γ and TNF-α levels in the culture supernatant. Consistently, a significant increase in IFN-γ-secreting splenocytes was observed in CRC mouse models and this parameter was inversely correlated with tumor volume. This finding aligned with previous reports indicating that intratumoral IFN-γ administration enhances immune cell infiltration and suppresses tumor growth (26,43-46). Furthermore, the capacity for IFN-γ secretion, a key T-cell activation marker (47), supports the notion that Exe-9 promotes tumor-specific $CD8^+$ T-cell activation and expansion. Collectively, these findings indirectly corroborated that Exe-9 enhances T-cell-mediated cytotoxicity in tumor cells. The present study findings support a T-cell-dependent mechanism based on CD8 infiltration, IFN-γ ELISpot responses and the lack of effect in nude mice; however, the present study acknowledges that detailed flow cytometry was not performed to assess T-cell activation, exhaustion markers or comprehensive tumor immune microenvironment profiling. Future studies should incorporate multiparameter flow cytometry and immune cell profiling to more precisely delineate how GLP-1R antagonism modulates T-cell functional states and tumor-infiltrating immune subsets. Notwithstanding this limitation, the present study findings provide indirect evidence that Exe-9 enhances T-cell-mediated cytotoxicity.

In addition to demonstrating the antitumor efficacy of GLP-1R antagonists as monotherapy for CRC, to the best of our knowledge, the present study provided the first direct evidence that combining a GLP-1R antagonist with anti-PD-1 therapy produces a synergistic antitumor effect. Specifically, mice receiving the combination treatment exhibited significantly reduced tumor volumes and weights compared with those treated with either agent alone. The therapeutic

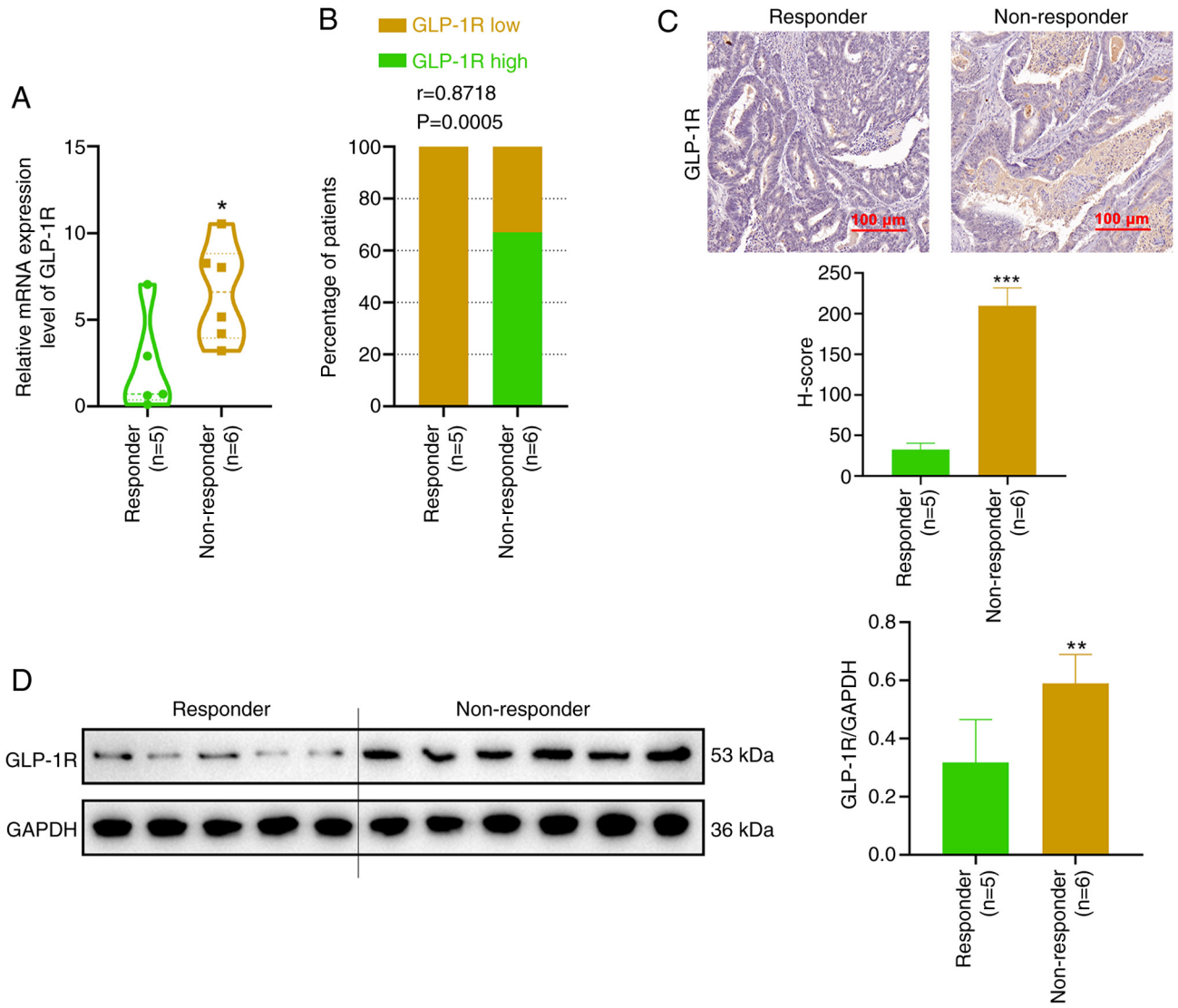

Figure 5. High GLP-1R expression correlates with reduced efficacy of anti-programmed cell death protein 1 immunotherapy in patients with CRC. Tumor specimens were collected from 11 patients with CRC treated with immune checkpoint inhibitors and subsequently categorized into responder (n=5) and non-responder (n=6) based on therapeutic outcomes. (A) Quantitative polymerase chain reaction analysis was performed to measure the mRNA expression levels of GLP-1R in tumor tissues. (B) Patients were further stratified into high and low receptor expression groups based on the median expression value. Pearson's correlation analysis was conducted to evaluate the relationship between receptor expression and treatment responsiveness. (C) Representative immunohistochemical images (scale bar, 100 μm) and (D) western blotting analysis illustrates the protein expression of GLP-1R in responders and non-responders. Data are presented as mean ± SEM. *P<0.05, **P<0.01 and ***P<0.001. GLP-1R, glucagon-like peptide-1 receptor; CRC, colorectal cancer.

rationale behind the use of ICIs, such as anti-PD-1/PD-L1 or anti-cytotoxic T-lymphocyte-associated antigen-4 antibodies, is based on their ability to block inhibitory signals from tumor cells that dampen T-cell activity, restoring T-cell-mediated antitumor responses. However, immunotherapy has exhibited limited efficacy in CRC primarily due to the reduced neoantigen burden of tumor cells, which hampers CD8^{+} T-cell activation and expansion as well as immunosuppressive factors present within the tumor microenvironment (48,49). Therefore, enhancing T-cell activity is considered a promising strategy in augmenting the effects of ICIs. For instance, CXCL10 overexpression increases CD8^{+} T-cell infiltration, sensitizing colorectal tumors to combined cetuximab and anti-PD-1 therapy (50). N-acetylcysteine induces differentiation of CD8^{+} T cell subpopulations, synergizing with anti-PD-1 antibodies to inhibit CRC progression in murine models (51). Similarly, the present study findings revealed that Exe-9, by antagonizing GLP-1R, enhances CD8^{+} T cell infiltration, activation and cytotoxic efficacy. This mechanism may help in overcoming the limitations of ICIs in treating CRC, particularly in 'cold tumor' settings and suggests a novel therapeutic target. Furthermore, the present *in vitro* and *in vivo* data were corroborated by clinical sample analyses, which revealed that high GLP-1R expression in patients with CRC undergoing ICI therapy was closely associated with a poor treatment response, underscoring the potential of GLP-1R as a negative predictive biomarker in immunotherapy. These findings are consistent with emerging reports identifying GLP-1R as a negative costimulatory signal in T cells (26,52), providing biological plausibility for its role as a therapeutic target and predictive biomarker.

Beyond T-cell co-stimulation, GLP-1R signaling has been associated with inflammatory regulation. Multiple studies have reported that GLP-1R activation dampens pro-inflammatory signaling pathways (53,54) and studies have identified GLP-1R as a negative costimulatory molecule in T cells, suggesting that antagonism may relieve this suppression and enhance effector T cell [T helper 1 cell (Th1)-type] responses (26,38,39). Consistent with this, the present study findings of increased IFN-γ secretion suggest that GLP-1R blockade may promote a Th1-skewed immune milieu, which is key to effective anti-tumor immunity.

Despite these promising results, the present study had certain limitations. First, the relatively small sample size in animal and clinical analyses may limit the generalizability of the present study findings. Second, exploratory analyses of The Cancer Genome Atlas CRC bulk RNA-sequencing did not reveal a strong correlation between GLP-1R expression and immune infiltration due to the low GLP-1R signal in these datasets (55,56). Hence, validation relies on larger IHC/qPCR-based cohorts and high-resolution single-cell or spatial datasets. Furthermore, the precise molecular mechanisms underlying the observed synergistic interaction between GLP-1R antagonism and immune checkpoint inhibition remain to be elucidated. Lastly, the long-term efficacy and safety of this combinatorial approach require further investigation in larger preclinical studies and clinical trials.

Translational challenges need to be considered. In the present preclinical study, Exe-9 was administered intratumorally, which is not a practical clinical route for most patients with CRC. Therefore, future studies should explore systemic delivery strategies, such as intravenous or subcutaneous administration and evaluate their pharmacokinetics and biodistribution. In addition, because GLP-1 signaling is closely associated with glucose metabolism and gastrointestinal function, GLP-1R antagonism may have metabolic side effects, including hyperglycemia or altered insulin responses. Careful preclinical safety assessments and early-phase clinical trials are required to determine tolerability. Notably, whether these effects extend to advanced or metastatic CRC remains to be elucidated, underscoring the need for validation in larger late-stage patient cohorts to determine the true clinical applicability. Lastly, future directions include the development of clinically feasible GLP-1R antagonists, the identification of predictive biomarkers to guide patient selection and the integration of this approach into rational combinatorial immunotherapy regimens.

In summary, the present study revealed that the GLP-1R antagonist Exe-9 significantly enhances T-cell-mediated cytotoxicity against CRC and when combined with ICIs, producing a synergistic antitumor effect. Clinical correlations indicate a negative association between GLP-1R expression and the efficacy of anti-PD-1 therapy. These findings highlight the potential of GLP-1R antagonism as a complementary strategy in improving immunotherapy outcomes in patients with CRC in the future.

Acknowledgements

Not applicable.

Funding

The present study was supported by the Guangzhou Health Science and Technology Project (grant no. 20251A010102).

Availability of data and materials

The data generated in the present study may be requested from the corresponding author.

Authors' contributions

ZZ and FC designed the experiments. CZ and LL conducted the experiments. DL and GM analyzed the experimental results. ZZ wrote the manuscript. FC revised the manuscript accordingly. ZZ and CZ confirm the authenticity of all the raw data. All authors read and approved the final version of the manuscript.

Ethics approval and consent to participate

All experimental procedures involving animals and human tissues were approved by the Ethics Committee of Guangzhou Development District Hospital (approval no. F2024-030; Guangzhou, China). All animal experiments were approved by the Institutional Animal Care and Use Committee of Guangzhou Development District Hospital, Guangzhou, China. For human studies (approval no. F2024-030), peripheral blood or tumor tissues were collected from healthy donors and patients, respectively, after obtaining written informed consent, following the Declaration of Helsinki. The Institutional Review Board of the Guangzhou Development District Hospital approved the present study protocol.

Patient consent for publication

Not applicable.

Competing interests

The authors declare that they have no competing interests.

References

1. Bin JF, Chen LF, Wang Y, Ge H and Chen W: Bibliometric and visual analysis of global crc circular RNA research 2015-2023. Front Immunol 16: 1580405, 2025.
2. Tsukanov VV, Vasyutin AV, Kasparov EV and Tonkikh JL: Is the use of artificial intelligence the main stage for detecting polyps during colonoscopy? World J Gastroenterol 31: 106500, 2025.
3. Saha P, Ravanan P and Talwar P: A multi-omics exploration of PPARG activation in colon cancer: Kinases featuring a PPRE sequence within regulatory regions. Biol Direct 20: 68, 2025.
4. Kamara AA, He S, Joseph Fofanah A, Xu R and Chen Y: MDPNet: Multiscale dynamic Polyp-focus network for enhancing medical image polyp segmentation. IEEE Trans Med Imaging 44: 5208-5220, 2025.
5. Araghi M, Soerjomataram I, Jenkins M, Brierley J, Morris E, Bray F and Arnold M: Global trends in colorectal cancer mortality: Projections to the year 2035. Int J Cancer 144: 2992-3000, 2019.
6. Ghorbaninezhad F, Nour MA, Farzam OR, Saeedi H, Vanan AG, Bakhshivand M, Jafarlou M, Hatami-Sadr A and Baradaran B: The tumor microenvironment and dendritic cells: Developers of pioneering strategies in colorectal cancer immunotherapy? Biochim Biophys Acta Rev Cancer 1880: 189281, 2025.

7. Steup C, Kennel KB, Neurath MF, Fichtner-Feigl S and Greten FR: Current and emerging concepts for systemic treatment of metastatic colorectal cancer. Gut 74: 2070-2095, 2025.
8. Hossain MS, Karuniawati H, Jairoun AA, Urbi Z, Ooi DJ, John A, Lim YC, Kibria KK, Mohiuddin A and Ming LC: Colorectal cancer: A review of carcinogenesis, global epidemiology, current challenges, risk factors, preventive and treatment strategies. Cancers 14: 1732, 2022.
9. Nors J, Iversen LH, Erichsen R, Gotschalck KA and Andersen CL: Incidence of recurrence and time to recurrence in stage I to III colorectal cancer: A nationwide Danish cohort study. JAMA Oncol 10: 54-62, 2024.
10. American Cancer Society. Cancer Facts & Figures 2024. Atlanta, GA, American Cancer Society, 2024.
11. Sabbatino F, Liguori L, Pepe S and Ferrone S: Immune checkpoint inhibitors for the treatment of melanoma. Expert Opin Biol Ther 22: 563-576, 2022.
12. Zhou F, Qiao M and Zhou C: The cutting-edge progress of immune-checkpoint blockade in lung cancer. Cell Mol Immunol 18: 279-293, 2021.
13. Makaremi S, Asadzadeh Z, Hemmat N, Baghbanzadeh A, Sgambato A, Ghorbaninezhad F, Safarpour H, Argentiero A, Brunetti O, Bernardini R, *et al*: Immune checkpoint inhibitors in colorectal cancer: Challenges and future prospects. Biomedicines 9: 1075, 2021.
14. Emambux S, Tachon G, Junca A and Tougeron D: Results and challenges of immune checkpoint inhibitors in colorectal cancer. Expert Opin Biol Ther 18: 561-573, 2018.
15. Ros J, Balconi F, Baraibar I, Saoudi Gonzalez N, Salva F, Tabernero J and Elez E: Advances in immune checkpoint inhibitor combination strategies for microsatellite stable colorectal cancer. Front Oncol 13: 1112276, 2023.
16. Trujillo JM, Nuffer W and Smith BA: GLP-1 receptor agonists: An updated review of head-to-head clinical studies. Ther Adv Endocrinol Metab 12: 2042018821997320, 2021.
17. Zheng Z, Zong Y, Ma Y, Tian Y, Pang Y, Zhang C and Gao J: Glucagon-like peptide-1 receptor: Mechanisms and advances in therapy. Signal Transduct Target Ther 9: 234, 2024.
18. del Olmo-Garcia MI and Merino-Torres JF: GLP-1 receptor agonists and cardiovascular disease in patients with type 2 diabetes. J Diabetes Res 2018: 4020492, 2018.
19. Yabut JM and Drucker DJ: Glucagon-like peptide-1 receptor-based therapeutics for metabolic liver disease. Endocr Rev 44: 14-32, 2023.
20. Halloum W, Dughem YA, Beier D and Pellesi L: Glucagon-like peptide-1 (GLP-1) receptor agonists for headache and pain disorders: A systematic review. J Headache Pain 25: 112, 2024.
21. Gala K, Camilleri M, Goyal M, Ohri A, Marek G and Ravi K: Glucagon-like Peptide-1 receptor agonist use is associated with and may lead to esophageal motility abnormalities. Clin Gastroenterol Hepatol: Nov 8, 2025 (Epub ahead of print). doi: 10.1016/j.cgh.2025.11.003.
22. Saha B, Kamalumpundi V and Codipilly DC: GLP1 and GIP receptor agonists: Effects on the gastrointestinal tract and management strategies for primary care physicians. Mayo Clin Proc: Dec 1, 2025 (Epub ahead of print). doi: 10.1016/j.mayocp.2025.09.017.
23. Chen J, Mei A, Wei Y, Li C, Qian H, Min X, Yang H, Dong L, Rao X and Zhong J: GLP-1 receptor agonist as a modulator of innate immunity. Front Immunol 13: 997578, 2022.
24. He Y, Xu B, Zhang M, Chen D, Wu S, Gao J, Liu Y, Zhang Z, Kuang J and Fang Q: Advances in GLP-1 receptor agonists for pain treatment and their future potential. J Headache Pain 26: 46, 2025.
25. Valencia-Rincón E, Rai R, Chandra V and Wellberg EA: GLP-1 receptor agonists and cancer: Current clinical evidence and translational opportunities for preclinical research. J Clin Invest 135: e194743, 2025.
26. Rode AK, Buus TB, Mraz V, Al-Jaberi FAH, Lopez DV, Ford SL, Hennen S, Eliasen IP, Klewe IV, Gharehdaghi L, *et al*: Induced human regulatory T cells express the glucagon-like peptide-1 receptor. Cells 11: 2587, 2022.
27. Paul MS and Ohashi PS: The roles of CD8+ T cell subsets in antitumor immunity. Trends Cell Biol 30: 695-704, 2020.
28. Liu YT and Sun ZJ: Turning cold tumors into hot tumors by improving T-cell infiltration. Theranostics 11: 5365, 2021.
29. Vafaei S, Zekiy AO, Khanamir RA, Zaman BA, Ghayourvahdat A, Azimizonuzi H and Zamani M: Combination therapy with immune checkpoint inhibitors (ICIs); a new frontier. Cancer Cell Int 22: 2, 2022.
30. Chiang CH, Song J, Chi KY, Chang YC, Xanthavanij N, Chang Y, Hsia YP, Chiang CH, Ghamari A, Reynolds KL, *et al*: Glucagon-like Peptide-1 agonists reduce cardiovascular events in cancer patients on immune checkpoint inhibitors. Eur J Cancer 216: 115170, 2025.
31. Quagliariello V, Canale ML, Bisceglia I, Iovine M, Giordano V, Giacobbe I, Scherillo M, Gabrielli D, Maurea C, Barbato M, *et al*: Glucagon-like peptide 1 receptor agonists in Cardio-oncology: Pathophysiology of cardiometabolic outcomes in cancer patients. Int J Mol Sci 25: 11299, 2024.
32. Vignarajah A, Kim S, Albliwi M, Ahn HM, Izda A, Naffa F, Vigneswaramoorthy N, Barot S and Shah G: Role of GLP-1 receptor agonists in managing cancer therapy-related cardiac dysfunction. J Am Heart Assoc 14: e040919, 2025.
33. Borner T, Pataro AM, Doebley SA, Furst CD, White AD, Gao SX, Chow A, Sanchez-Navarro MJ, Ghidewon MY, Halas JG, *et al*: Hypophagia and body weight loss by tirzepatide are accompanied by fewer GI adverse events compared to semaglutide in preclinical models. Sci Adv 11: eadu1589, 2025.
34. Eisenhauer EA, Therasse P, Bogaerts J, Schwartz LH, Sargent D, Ford R, Dancey J, Arbuck S, Gwyther S, Mooney M, *et al*: New response evaluation criteria in solid tumours: Revised RECIST guideline (version 1.1). Eur J Cancer 45: 228-247, 2009.
35. Wen Z, Luo D, Wang S, Rong R, Evers BM, Jia L, Fang Y, Daoud EV, Yang S, Gu Z, *et al*: Deep Learning-Based H-Score quantification of Immunohistochemistry-stained images. Mod Pathol 37: 100398, 2024.
36. Livak KJ and Schmittgen TD: Analysis of relative gene expression data using Real-time quantitative PCR and the 2(-Delta Delta C(T)) method. Methods 25: 402-408, 2001.
37. Islam MR, Akash S, Rahman MM, Nowrin FT, Akter T, Shohag S, Rauf A, Aljohani AS and Simal-Gandara J: Colon cancer and colorectal cancer: Prevention and treatment by potential natural products. Chem Biol Interact 368: 110170, 2022.
38. Ben Nasr M, Usuelli V, Dellepiane S, Seelam AJ, Fiorentino TV, D'Addio F, Fiorina E, Xu C, Xie Y, Balasubramanian HB, *et al*: Glucagon-like peptide 1 receptor is a T cell-negative costimulatory molecule. Cell Metab 36: 1302-1319.e12, 2024.
39. Wong CK, Yusta B, Koehler JA, Baggio LL, McLean BA, Matthews D, Seeley RJ and Drucker DJ: Divergent roles for the gut intraepithelial lymphocyte GLP-1R in control of metabolism, microbiota, and T cell-induced inflammation. Cell Metab 34: 1514-1531.e7, 2022.
40. Shilyansky JS, Chan CJ, Xiao S, Gribovskaja-Rupp I, Quelle DE, Howe JR, Dillon JS and Ear PH: GLP-1R agonist promotes proliferation of neuroendocrine neoplasm cells expressing GLP-1 receptors. Surgery 179: 108943, 2025.
41. Shabil M, Khatib MN, Ballal S, Bansal P, Tomar BS, Ashraf A, Kumar MR, Sinha A, Rawat P, Gaidhane AM, *et al*: Risk of hepatocellular carcinoma with Glucagon-like Peptide-1 receptor agonist treatment in patients: A systematic review and meta-analysis. BMC Endocr Disord 24: 246, 2024.
42. Koehler JA, Kain T and Drucker DJ: Glucagon-like peptide-1 receptor activation inhibits growth and augments apoptosis in murine CT26 colon cancer cells. Endocrinology 152: 3362-3372, 2011.
43. Tang Y, Wei J, Ge X, Yu C, Lu W, Qian Y, Yang H, Fu D, Fang Y, Zhou X, *et al*: Intratumoral injection of interferon gamma promotes the efficacy of anti-PD1 treatment in colorectal cancer. Cancer Lett 588: 216798, 2024.
44. Zhong FM, Yao FY, Yang YL, Liu J, Li MY, Jiang JY, Zhang N, Xu YM, Li SQ, Cheng Y, *et al*: Molecular subtypes predict therapeutic responses and identifying and validating diagnostic signatures based on machine learning in chronic myeloid leukemia. Cancer Cell Int 23: 61, 2023.
45. Xie Y, Lv Z, Wang Y, Ma J, Wei X, Zheng G and Wu J: Study on the efficacy of IFN-γ- and sPD-1-overexpressing BMSCs in enhancing immune effects for the treatment of lung adenocarcinoma. Front Immunol 16: 1554467, 2025.
46. Hogg GD, Weinstein AG, Kingston NL, Liu X, Dres OM, Kang LI, Lander VE, Kao YL, Ahmad F, Knolhoff BL, *et al*: Combined Flt3L and CD40 agonism restores dendritic cell-driven T cell immunity in pancreatic cancer. Sci Immunol 10: eadp3978, 2025.
47. Andrews LP, Butler SC, Cui J, Cillo AR, Cardello C, Liu C, Brunazzi EA, Baessler A, Xie B, Kunning SR, *et al*: LAG-3 and PD-1 synergize on CD8+ T cells to drive T cell exhaustion and hinder autocrine IFN-γ-dependent anti-tumor immunity. Cell 187: 4355-4372.e22, 2024.
48. Zhou C, Cheng X and Tu S: Current status and future perspective of immune checkpoint inhibitors in colorectal cancer. Cancer Lett 521: 119-129, 2021.

49. Sahin IH, Ciombor KK, Diaz LA, Yu J and Kim R: Immunotherapy for microsatellite stable colorectal cancers: Challenges and novel therapeutic avenues. Am Soc Clin Oncol Educ Book 42: 1-12, 2022.
50. Yan W, Qiu L, Yang M, Xu A, Ma M, Yuan Q, Ma X, Liang W, Li X and Lu Y: CXCL10 mediates CD8+ T cells to facilitate vessel normalization and improve the efficacy of cetuximab combined with PD-1 checkpoint inhibitors in colorectal cancer. Cancer Lett 567: 216263, 2023.
51. Zhou W, Qu M, Yue Y, Zhong Z, Nan K, Sun X, Wu Q, Zhang J, Chen W and Miao C: Acetylcysteine synergizes PD-1 blockers against colorectal cancer progression by promoting TCF1+ PD1+ CD8+ T cell differentiation. Cell Commun Signal 22: 503, 2024.
52. Zhu C, Lai Y, Liu C, Teng L, Zhu Y, Lin X, Fu X, Lai Q, Liu S, Zhou X and Fang Y: Comprehensively prognostic and immunological analyses of GLP-1 signaling-related genes in pan-cancer and validation in colorectal cancer. Front Pharmacol 15: 1387243, 2024.
53. Alharbi SH: Anti-inflammatory role of glucagon-like peptide 1 receptor agonists and its clinical implications. Ther Adv Endocrinol Metab 15: 20420188231222367, 2024.
54. Wong S, Le GH, Dri CE, Teopiz KM and McIntyre RS: Evaluating biased agonism of glucagon-like peptide-1 (GLP-1) receptors to improve cellular bioenergetics: A systematic review. Diabetes Obes Metab 27: 6105-6115, 2025.
55. Wong CK, Yusta B, Tong JCL, Broichhagen J, Hodson DJ and Drucker DJ: Reassessment of antibody-based detection of the murine T cell GLP-1 receptor. Cell Metab 37: 1783-1788, 2025.
56. Pang J, Feng JN, Ling W and Jin T: The anti-inflammatory feature of glucagon-like peptide-1 and its based diabetes drugs-Therapeutic potential exploration in lung injury. Acta Pharm Sin B 12: 4040-4055, 2022.